Initial eccentricity fluctuations and their relation to higher-order flow harmonics

Roy A. Lacey,[1,2,*] Rui Wei,[1] J. Jia,[1,2] N. N. Ajitanand,[1] J. M. Alexander,[1] and A. Taranenko[1]
[1]*Department of Chemistry, Stony Brook University, Stony Brook, New York 11794-3400, USA*
[2]*Physics Department, Brookhaven National Laboratory, Upton, New York 11973-5000, USA*
(Received 27 September 2010; published 8 April 2011)

Monte Carlo simulations are used to compute the centrality dependence of the participant eccentricities (ε_n) in Au + Au collisions for the two primary models currently employed for eccentricity estimates—the Glauber and the factorized Kharzeev-Levin-Nardi (fKLN) models. They suggest specific testable predictions for the magnitude and centrality dependence of the flow coefficients v_n, respectively measured relative to the event planes Ψ_n. They also indicate that the ratios of several of these coefficients may provide an additional constraint for distinguishing between the models. Such a constraint could be important for a more precise determination of the specific viscosity of the matter produced in heavy ion collisions.

DOI: 10.1103/PhysRevC.83.044902 PACS number(s): 25.75.Ld, 25.75.Dw, 25.75.Gz

Collective flow continues to play a central role in ongoing efforts to characterize the transport properties of the strongly interacting matter produced in heavy ion collisions at the Relativistic Heavy Ion Collider (RHIC) [1–16]. An experimental manifestation of this flow is the anisotropic emission of particles in the plane transverse to the beam direction [17,18]. This anisotropy can be characterized by the even-order Fourier coefficients,

$$v_n = \langle e^{in(\phi_p - \Psi_{\rm RP})} \rangle, \quad n = 2, 4, \ldots, \tag{1}$$

where ϕ_p is the azimuthal angle of an emitted particle, $\Psi_{\rm RP}$ is the azimuth of the reaction plane, and the brackets denote averaging over particles and events [19]. Characterization has also been made via the pairwise distribution in the azimuthal angle difference ($\Delta\phi = \phi_1 - \phi_2$) between particles [17,20,21]:

$$\frac{dN^{\rm pairs}}{d\Delta\phi} \propto \left[1 + \sum_{n=1} 2v_n^2 \cos(n\Delta\phi)\right]. \tag{2}$$

Anisotropic flow is understood to result from an asymmetric hydrodynamiclike expansion of the medium produced by the two colliding nuclei. That is, the spacial asymmetry of the produced medium drives uneven pressure gradients in and out of the reaction plane and, hence, a momentum anisotropy of the particles is emitted about this plane. This mechanistic picture is well supported by the observation that the measured anisotropy for hadron $p_T \lesssim 2$ GeV/c can be described by relativistic hydrodynamics [5,10,12,14,15,22–31].

The differential Fourier coefficients $v_2(N_{\rm part})$ and $v_2(p_T)$ have been extensively studied in Au + Au collisions at the RHIC [20,32–38]. One reason for this has been the realization that these elliptic flow coefficients are sensitive to various transport properties of the expanding hot medium [5–7,9,11,13,23,39–41]. Indeed, considerable effort has been and is being devoted to the quantitative extraction of the specific shear viscosity η/s (i.e., the ratio of shear viscosity η to entropy density s) via comparisons to viscous relativistic hydrodynamic simulations [9–12,14,15,30], transport model calculations [6,13,42], and hybrid approaches that involve the parametrization of scaling violations to ideal hydrodynamic behavior [7,16,40,43,44]. The initial eccentricity of the collision zone and its associated fluctuations has proven to be an essential ingredient for these extractions.

Experimental measurements of the eccentricity have not been possible to date. Consequently, much reliance has been placed on the theoretical estimates obtained from the overlap geometry of the collision zone, specified by the impact parameter b or the number of participants $N_{\rm part}$ [31,34,43,45–52]. For these estimates, the geometric fluctuations associated with the positions of the nucleons in the collision zone serve as the underlying cause of the initial eccentricity fluctuations. That is, the fluctuations of the positions of the nucleons lead to fluctuations of the so-called participant plane (from one event to another) which result in larger values for the eccentricities (ε) referenced to this plane.

The magnitude of these fluctuations are, of course, model dependent, and this leads to different predictions for the magnitude of the eccentricity. More specifically, the ε_2 values obtained from the Glauber [34,53] and the factorized Kharzeev-Levin-Nardi (fKLN) [54,55] models (the two primary models currently employed for eccentricity estimates) give results that differ by as much as ∼25% [56,57]—a difference that leads to an approximate factor of 2 uncertainty in the extracted η/s value [9,16]. Thus, a more precise extraction of η/s requires a clever experimental technique that can measure the eccentricity and/or the development of experimental constraints that can facilitate the requisite distinction between the models used to calculate eccentricity.

Recently, significant attention has been given to the study of the influence of initial geometry fluctuations on higher-order eccentricities $\varepsilon_{n,n\geqslant 3}$ [30,31,47,50–52,58–60], with an eye toward a better understanding of how such fluctuations manifest into the harmonic flow correlations characterized by v_n (for odd and even n), and whether they can yield constraints that could serve to pin down the "correct" model for eccentricity determination. For the latter, the magnitudes of ε_n and its detailed centrality dependence are critical. Therefore, it is essential to resolve the substantial differences

*roy.lacey@stonybrook.edu

in the ε_n values reported and used by different authors [30,31,47,50–52,58–60].

Here, we argue that the magnitudes and trends for the eccentricities ε_n imply specific testable predictions for the magnitude and centrality dependence of the flow coefficients v_n, measured relative to their respective event planes Ψ_n. We also show that the values for ε_n obtained for the Glauber [34,53] and fKLN [54,55] models indicate sizable model-dependent differences that could manifest in experimentally detectable differences in the centrality dependence of the ratios $v_3/(v_2)^{3/2}$, $v_4/(v_2)^2$, and $v_2/v_{n,n\geqslant 3}$. Such a constraint could be important for a more precise determination of the specific viscosity of the hot and dense matter produced in heavy ion collisions.

I. ECCENTRICITY SIMULATIONS

Monte Carlo (MC) simulations were used to calculate event-averaged eccentricities (denoted here as ε_n) in Au + Au collisions, within the framework of the Glauber (MC-Glauber) and fKLN (MC-KLN) models. For each event, the spatial distribution of nucleons in the colliding nuclei were generated according to the Woods-Saxon function:

$$\rho(\mathbf{r}) = \frac{\rho_0}{1 + e^{(\mathrm{r}-R_0)/d}}, \tag{3}$$

where $R_0 = 6.38$ fm is the radius of the Au nucleus and $d = 0.53$ fm is the diffuseness parameter.

For each collision, the values for N_{part} and the number of binary collisions N_{coll} were determined within the Glauber ansatz [53]. The associated ε_n values were then evaluated from the two-dimensional profile of the density of sources in the transverse plane $\rho_s(\mathbf{r}_\perp)$, using modified versions of MC-Glauber [53] and MC-KLN [55], respectively.

For each event, we compute an event shape vector S_n and the azimuth of the rotation angle Ψ_n for the nth harmonic of the shape profile [47,50],

$$S_{nx} \equiv S_n \cos(n\Psi_n) = \int d\mathbf{r}_\perp \rho_s(\mathbf{r}_\perp)\omega(\mathbf{r}_\perp)\cos(n\phi), \tag{4}$$

$$S_{ny} \equiv S_n \sin(n\Psi_n) = \int d\mathbf{r}_\perp \rho_s(\mathbf{r}_\perp)\omega(\mathbf{r}_\perp)\sin(n\phi), \tag{5}$$

$$\Psi_n = \frac{1}{n}\tan^{-1}\left(\frac{S_{ny}}{S_{nx}}\right), \tag{6}$$

where ϕ is the azimuthal angle of each source and the weights $\omega(\mathbf{r}_\perp) = {\mathbf{r}_\perp}^2$ and $\omega(\mathbf{r}_\perp) = {\mathbf{r}_\perp}^n$ are used in respective calculations. Here, it is important to note that the substantial differences reported for ε_n in Refs. [30,31,47,50–52,58–60] are largely due to the value of $\omega(\mathbf{r}_\perp)$ employed.

The eccentricities were calculated as

$$\varepsilon_n = \langle \cos n(\phi - \Psi_n)\rangle \tag{7}$$

and

$$\varepsilon_n^* = \langle \cos n(\phi - \Psi_m)\rangle, \quad n \neq m, \tag{8}$$

where the brackets denote averaging over sources and events belonging to a particular centrality or impact parameter range; the starred notation is used here to distinguish the nth order moments obtained relative to an event plane of a different order Ψ_m.

For the MC-Glauber calculations, an additional entropy density weight was applied reflecting the combination of spatial coordinates of participating nucleons and binary collisions [48,56]:

$$\rho_s(\mathbf{r}_\perp) \propto \left[\frac{(1-\alpha)}{2}\frac{dN_{\mathrm{part}}}{d^2\mathbf{r}_\perp} + \alpha\frac{dN_{\mathrm{coll}}}{d^2\mathbf{r}_\perp}\right], \tag{9}$$

where $\alpha = 0.14$ was constrained by multiplicity measurements as a function of N_{part} for Au + Au collisions [61]. These procedures take account of the eccentricity fluctuations that stem from the event-by-event misalignment between the short axis of the "almond-shaped" collision zone and the impact parameter. Note that ε_n [cf. Eq. (7)] corresponds to v_n measurements relative to the so-called participant planes [34,53]. That is, each harmonic ε_n is evaluated relative to the principal axis determined by maximizing the nth moment. This is analogous to the measurement of v_n with respect to the nth order event-plane in actual experiments [62]. It, however, contrasts recent experimental measurements in which a higher-order coefficient (v_4) has been measured with respect to a lower-order event plane (Ψ_2) [38,63]. Note as well that we have established that the angles Ψ_n for the odd and even harmonics are essentially uncorrelated for the N_{part} range of interest to this study.

A. Results for $\omega(\mathbf{r}_\perp) = {\mathbf{r}_\perp}^2$ and $\omega(\mathbf{r}_\perp) = {\mathbf{r}_\perp}^n$

Figure 1 shows a comparison of $\varepsilon_{n,n\leqslant 6}$ vs N_{part} for $\omega(\mathbf{r}_\perp) = {\mathbf{r}_\perp}^2$, for MC-Glauber (a) and MC-KLN (b) models for Au + Au collisions. The solid and open symbols indicate the results for the even and odd harmonics, respectively. For this weighting scheme, ε_n is essentially the same for $n \geqslant 3$

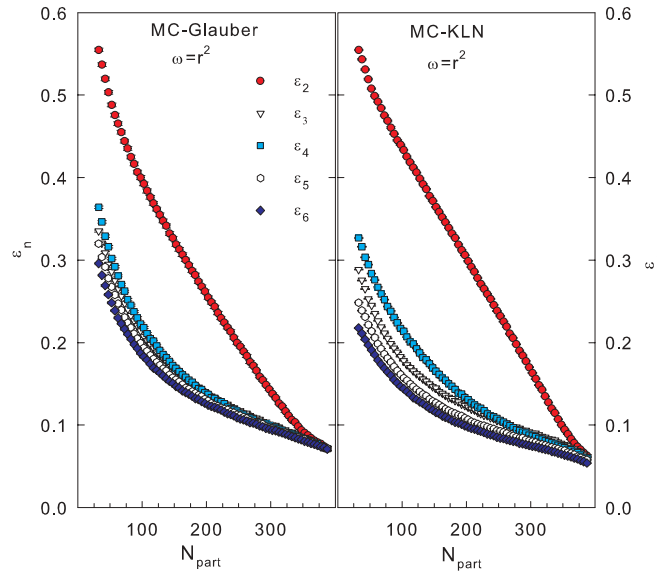

FIG. 1. (Color online) Calculated values of $\varepsilon_{n,n\leqslant 6}$ vs N_{part} for $\omega(\mathbf{r}_\perp) = {\mathbf{r}_\perp}^2$ for MC-Glauber (a) and MC-KLN (b) for Au + Au collisions. The open and solid symbols indicate the results for odd and even harmonics, respectively.

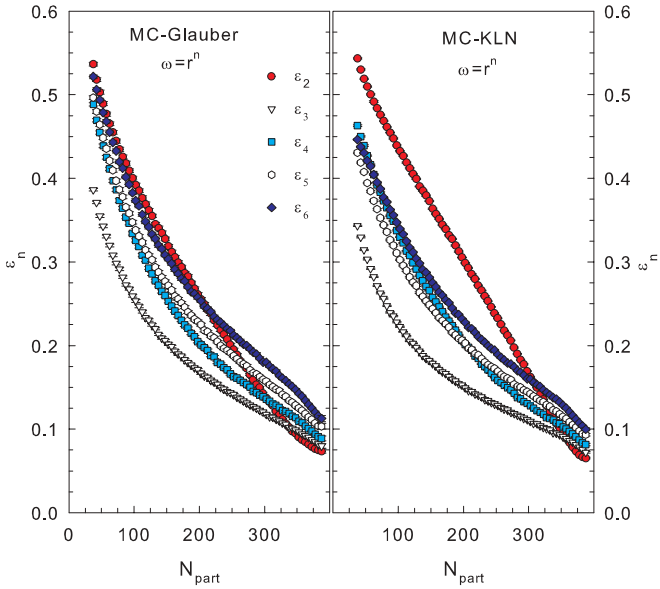

FIG. 2. (Color online) Same as Fig. 1 for $\omega(\mathbf{r}_\perp) = \mathbf{r}_\perp{}^n$.

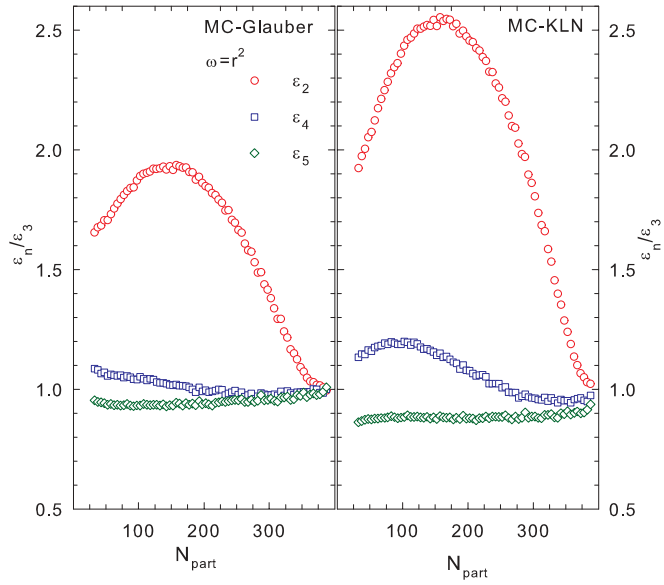

FIG. 3. (Color online) Comparison of $\varepsilon_{2,4,5}/\varepsilon_3$ vs $N_{\rm part}$ for Au + Au collisions. Results are shown for MC-Glauber (a) and MC-KLN (b) calculations.

and has magnitudes which are significantly less than that for ε_2, except in very central collisions where the effects of fluctuation dominate the magnitude of $\varepsilon_{n,n\geqslant 2}$. Note the approximate $1/\sqrt{(N_{\rm part})}$ dependence for $\varepsilon_{n,n\geqslant 3}$. The smaller magnitudes for $\varepsilon_{n,n\geqslant 3}$ (with larger spread) apparent in Fig. 1(b) can be attributed to the sharper transverse density distributions for MC-KLN.

Figure 2 shows a similar comparison of $\varepsilon_{n,n\leqslant 6}$ vs $N_{\rm part}$ for calculations performed with the weight $\omega(\mathbf{r}_\perp) = \mathbf{r}_\perp{}^n$. This weighting results in an increase in the sensitivity to the outer regions of the transverse density distributions. Consequently, the overall magnitudes for $\varepsilon_{n,n\geqslant 3}$ are larger than those shown in Fig. 1. This weighting also leads to a striking difference in the relative magnitudes of $\varepsilon_{n,n\geqslant 2}$ for MC-Glauber (a), MC-KLN (b), and the results for $\omega(\mathbf{r}_\perp) = \mathbf{r}_\perp{}^2$ shown in Fig. 1.

II. ECCENTRICITY RATIOS

The magnitudes and trends of the calculated eccentricities shown in Figs. 1 and 2 are expected to influence the measured values of v_n. To estimate this influence, we first assume that the resulting anisotropic flow is directly proportional to the initial eccentricity, as predicted by perfect fluid hydrodynamics. Here, our tacit assumption is that a possible influence from the effects of a finite viscosity (η/s) is small because current estimates indicate that η/s is small [4,6,7,9–16,30,40,43,44]—of the same magnitude as for the conjectured lower bound $\eta/s = 1/4\pi$, by Kovtun, Son and Starinets [64].

Figure 1 indicates specific testable predictions for the relative influence of $\varepsilon_{n,n\geqslant 2}$ on the magnitudes of $v_{n,n\geqslant 2}$. That is, (i) ε_2 should have a greater influence than $\varepsilon_{n,n\geqslant 3}$ in noncentral collisions, (ii) the respective influence of $\varepsilon_{n,n\geqslant 3}$ on the values for $v_{n,n\geqslant 3}$ should be similar irrespective of centrality, and (iii) the ratios $v_{4,5,6}/v_3$ should follow a specific centrality dependence due to the influence of $\varepsilon_{4,5,6}/\varepsilon_3$. Such a dependence is illustrated in Fig. 3, where we show the centrality dependence of the ratios $\varepsilon_{2,4,5}/\varepsilon_3$, obtained for MC-Glauber (a) and MC-KLN (b) calculations. They suggest that, if MC-Glauber-like eccentricities, with weight $\omega(\mathbf{r}_\perp) = \mathbf{r}_\perp{}^2$, are the relevant eccentricities for Au + Au collisions, then the measured ratio v_2/v_3 should increase by a factor of $\approx$2, from central to midcentral collisions ($N_{\rm part} \sim 350$–150). For $N_{\rm part} \lesssim 150$, Fig. 2(a) shows that the ratio v_2/v_3 could even show a modest decrease. The eccentricity ratios involving the higher harmonics suggest that, if they are valid, the measured values of $v_{4,5,6}/v_3$ should show little, if any, dependence on centrality, irrespective of their magnitudes.

The ratios $\varepsilon_{2,4,5}/\varepsilon_3$ obtained for MC-KLN calculations are shown in Fig. 3(b). While they indicate qualitative trends which are similar to the ones observed in Fig. 3(a), their magnitudes and their detailed dependence on centrality are different. Therefore, if the qualitative trends discussed earlier were indeed found in the data, then these differences suggest that precision measurements of the centrality dependence of the relative ratios for v_2/v_3, v_4/v_3, $v_5/v_3, \ldots$ for several p_T selections, could provide a constraint for aiding the distinction between fKLN-like and Glauber-like initial collision geometries. Specifically, smaller (larger) values of the relative ratios are to be expected for v_2/v_3 and v_4/v_3 for Glauber-like (fKLN-like) initial geometries. Note the differences in the expected centrality dependencies as well.

Figure 4 compares the eccentricity ratios $\varepsilon_{2,4,5}/\varepsilon_3$ obtained for the MC-Glauber (a) and MC-KLN (b) calculations with the weight $\omega(\mathbf{r}_\perp) = \mathbf{r}_\perp{}^n$. The magnitudes of these ratios and their centrality dependencies are distinct for the MC-Glaber and MC-KLN calculations. They are also quite different from the ratios shown in Fig. 3. This suggests that precision measurements of the centrality dependence of the relative ratios v_2/v_3, v_4/v_3, $v_5/v_3, \ldots$ (for several p_T selections) should not only allow a clear distinction between MC-Glauber

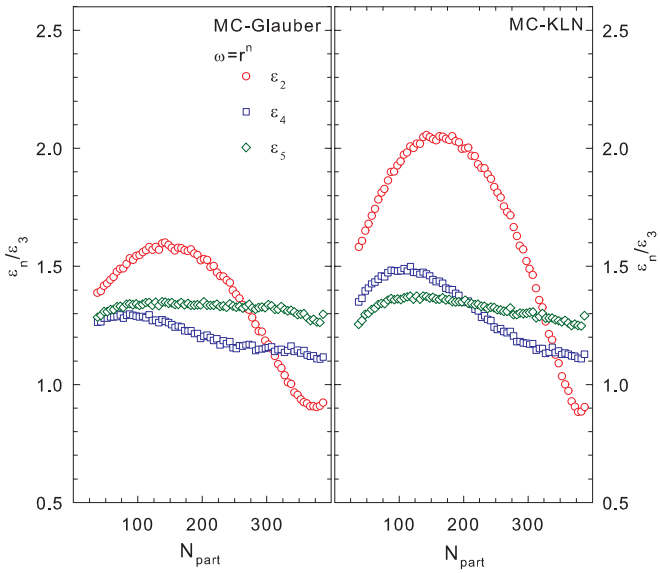

FIG. 4. (Color online) Same as Fig. 3 for $\omega(\mathbf{r}_\perp) = \mathbf{r}_\perp{}^n$.

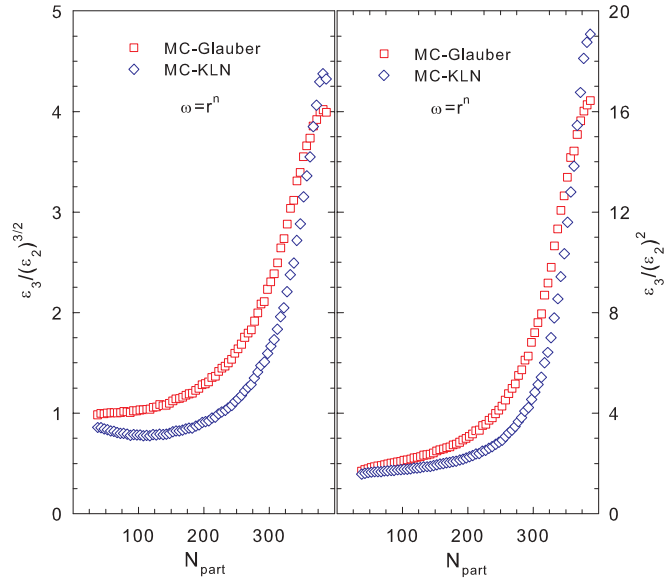

FIG. 6. (Color online) Same as Fig. 5 for $\omega(\mathbf{r}_\perp) = \mathbf{r}_\perp{}^n$.

and MC-KLN initial geometries but also a distinction between the $\omega(\mathbf{r}_\perp) = \mathbf{r}_\perp{}^2$ and $\omega(\mathbf{r}_\perp) = \mathbf{r}_\perp{}^n$ weighting methods.

A finite viscosity will influence the magnitudes of v_n. Thus, for a given p_T selection, the measured ratios for v_2/v_3, v_4/v_3, $v_5/v_3, \ldots$ will be different from the eccentricity ratios shown in Figs. 3 and 4. Note as well that, even for ideal hydrodynamics, the predicted magnitude of v_4/ε_4 is only a half of that for v_2/ε_2 [59]. Nonetheless, the rather distinct centrality-dependent eccentricity patterns exhibited in Figs. 3 and 4 suggest that measurements of the ratios of these flow harmonics should still allow a distinction between MC-Glauber and MC-KLN initial geometries, as well as a distinction between the two weighting methods.

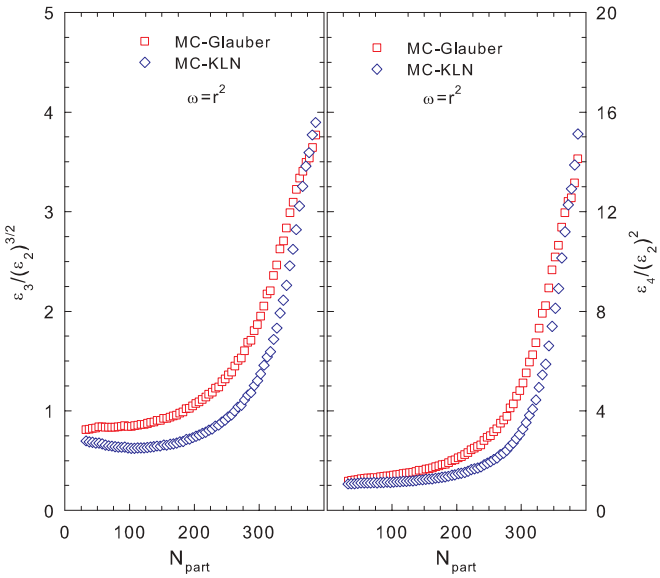

FIG. 5. (Color online) Comparison of $\varepsilon_3/(\varepsilon_2)^{3/2}$ vs $N_{\rm part}$ (a) and $\varepsilon_4/(\varepsilon_2)^2$ vs $N_{\rm part}$ (b) for MC-Glauber and MC-KLN initial geometries (as indicated) for Au + Au collisions.

The ratios $v_3/(v_2)^{3/2}$ and $v_4/(v_2)^2$ have been recently found to scale with p_T [65], suggesting a reduction in the influence of viscosity on them. Thus, the measured ratios $v_n/(v_2)^{n/2}$ could give a more direct indication of the centrality-dependent influence of $\varepsilon_n/(\varepsilon_2)^{n/2}$ on $v_n/(v_2)^{n/2}$. The open symbols in Figs. 5 and 6 indicate a substantial difference between the ratios $\varepsilon_3/(\varepsilon_2)^{3/2}$ (a) and $\varepsilon_4/(\varepsilon_2)^2$ (b) for the MC-Glauber and MC-KLN geometries as indicated. Note as well that the ratios in Fig. 6 are substantially larger than those in Fig. 5. The latter difference reflects the different weighting schemes used, i.e., $\omega(\mathbf{r}_\perp) = \mathbf{r}_\perp{}^n$ and $\omega(\mathbf{r}_\perp) = \mathbf{r}_\perp{}^2$, respectively. Interestingly, the ratios for $\varepsilon_4/(\varepsilon_2)^2$ imply much larger measured ratios for $v_4/(v_2)^2$ than the value of 0.5 predicted by perfect fluid hydrodynamics (without fluctuations) [66,67]. However, they show qualitative trends that are similar to those for the measured ratios $v_4/(v_2)^2$, obtained for v_4 evaluations relative to the Ψ_2 plane [38,63]. The relatively steep rise of the ratios in Figs. 5 and 6 (albeit steeper for MC-Glauber) can be attributed to the larger influence that fluctuations have on the higher harmonics. Note that these are the same fluctuations that give rise to the "anomalously low" values of ε_4 evaluated with respect to Ψ_2 in central collisions [50].

Figures 3–6 suggest that measurements of the centrality dependence of the ratios $v_3/(v_2)^{3/2}$ and $v_4/(v_2)^2$, in conjunction with those for v_2/v_3, v_4/v_3, $v_5/v_3 \ldots$, may provide a robust constraint for the role of initial eccentricity fluctuations, as well as an additional handle for making a distinction between Glauber-like and fKLN-like initial geometries. These measurements could also lend insight, as well as place important constraints for the degree to which a small value of η/s and/or the effects of thermal smearing modulate the higher order flow harmonics [compared to v_2] as has been suggested [31,52,60].

III. SUMMARY

In summary, we have presented results for the initial eccentricities $\varepsilon_{n,n\leqslant 6}$ for Au + Au collisions with different weighting

schemes for the two primary models currently employed for eccentricity estimates at the RHIC. The calculated values of $\varepsilon_{n,n\leqslant 6}$, which are expected to influence the measured flow harmonics v_n, suggest that measurements of the centrality dependence of $v_2/(v_3)$, v_4/v_3, $v_3/(v_2)^{3/2}$, $v_4/(v_2)^2$, etc. could provide stringent constraints for validating the predicted influence of eccentricity fluctuations on v_n, as well as an important additional handle for making a distinction between Glauber-like and fKLN-like initial geometries. Measurements of v_n and their ratios are now required to exploit these simple tests.

ACKNOWLEDGMENTS

We thank Wojciech Broniowski for profitable discussions and invaluable model calculation cross checks. This research is supported by the US DOE under Contract DE-FG02-87ER40331.A008 and by the NSF under Grant PHY-1019387.

[1] M. Gyulassy and L. McLerran, Nucl. Phys. A **750**, 30 (2005).
[2] D. Molnar and P. Huovinen, Phys. Rev. Lett. **94**, 012302 (2005).
[3] R. A. Lacey *et al.*, Phys. Rev. Lett. **98**, 092301 (2007).
[4] A. Adare *et al.*, Phys. Rev. Lett. **98**, 172301 (2007).
[5] P. Romatschke and U. Romatschke, Phys. Rev. Lett. **99**, 172301 (2007).
[6] Z. Xu, C. Greiner, and H. Stocker, Phys. Rev. Lett. **101**, 082302 (2008).
[7] H.-J. Drescher, A. Dumitru, C. Gombeaud, and J.-Y. Ollitrault, Phys. Rev. C **76**, 024905 (2007).
[8] E. Shuryak, Prog. Part. Nucl. Phys. **62**, 48 (2009).
[9] M. Luzum and P. Romatschke, Phys. Rev. C **78**, 034915 (2008).
[10] H. Song and U. W. Heinz, J. Phys. G **36**, 064033 (2009).
[11] A. K. Chaudhuri, J. Phys. G **37**, 075011 (2010).
[12] K. Dusling and D. Teaney, Phys. Rev. C **77**, 034905 (2008).
[13] V. Greco, M. Colonna, M. Di Toro, and G. Ferini, Prog. Part. Nucl. Phys. **62**, 562 (2009).
[14] P. Bozek and I. Wyskiel, PoS **EPS-HEP-2009**, 039 (2009).
[15] G. S. Denicol, T. Kodama, and T. Koide, J. Phys. G **37**, 094040 (2010).
[16] R. A. Lacey *et al.*, Phys. Rev. C **82**, 034910 (2010).
[17] R. A. Lacey, Nucl. Phys. A **698**, 559 (2002).
[18] R. J. M. Snellings, Nucl. Phys. A **698**, 193 (2002).
[19] J.-Y. Ollitrault, Phys. Rev. D **46**, 229 (1992).
[20] K. Adcox *et al.*, Phys. Rev. Lett. **89**, 212301 (2002).
[21] A. Mocsy and P. Sorensen, arXiv:1008.3381 [hep-ph].
[22] U. Heinz and P. Kolb, Nucl. Phys. A **702**, 269 (2002).
[23] D. Teaney, Phys. Rev. C **68**, 034913 (2003).
[24] P. Huovinen, P. F. Kolb, U. W. Heinz, P. V. Ruuskanen, and S. A. Voloshin, Phys. Lett. B **503**, 58 (2001).
[25] T. Hirano and K. Tsuda, Phys. Rev. C **66**, 054905 (2002).
[26] R. Andrade *et al.*, Eur. Phys. J. A **29**, 23 (2006).
[27] C. Nonaka, N. Sasaki, S. Muroya, and O. Miyamura, Nucl. Phys. A **661**, 353 (1999).
[28] H. Niemi, K. J. Eskola, and P. V. Ruuskanen, Phys. Rev. C **79**, 024903 (2009).
[29] R. Peschanski and E. N. Saridakis, Phys. Rev. C **80**, 024907 (2009).
[30] H. Holopainen, H. Niemi, and K. J. Eskola, Phys. Rev. C **83**, 034901 (2011).
[31] B. Schenke, S. Jeon, and C. Gale, Phys. Rev. Lett. **106**, 042301 (2011).
[32] J. Adams *et al.*, Phys. Rev. Lett. **92**, 062301 (2004).
[33] S. S. Adler *et al.*, Phys. Rev. Lett. **91**, 182301 (2003).
[34] B. Alver *et al.*, Phys. Rev. Lett. **98**, 242302 (2007).
[35] S. Afanasiev *et al.* (PHENIX Collaboration), Phys. Rev. Lett. **99**, 052301 (2007).
[36] B. I. Abelev *et al.* (STAR Collaboration), Phys. Rev. C **77**, 054901 (2008).
[37] S. Afanasiev *et al.* (PHENIX Collaboration), Phys. Rev. C **80**, 024909 (2009).
[38] A. Adare *et al.* (PHENIX Collaboration), arXiv:1003.5586 [nucl-ex].
[39] U. W. Heinz and S. M. H. Wong, Phys. Rev. C **66**, 014907 (2002).
[40] R. A. Lacey and A. Taranenko, PoS **CFRNC2006**, 021 (2006).
[41] H. Song and U. W. Heinz, Phys. Rev. C **77**, 064901 (2008).
[42] D. Molnar and M. Gyulassy, Nucl. Phys. A **697**, 495 (2002).
[43] R. A. Lacey, A. Taranenko, and R. Wei, arXiv:0905.4368 [nucl-ex].
[44] H. Masui, J.-Y. Ollitrault, R. Snellings, and A. Tang, Nucl. Phys. A **830**, 463c (2009).
[45] M. Miller and R. Snellings, arXiv:nucl-ex/0312008.
[46] Y. Hama *et al.*, Phys. Atom. Nucl. **71**, 1558 (2008).
[47] W. Broniowski, P. Bozek, and M. Rybczynski, Phys. Rev. C **76**, 054905 (2007).
[48] T. Hirano and Y. Nara, Phys. Rev. C **79**, 064904 (2009).
[49] C. Gombeaud and J.-Y. Ollitrault, Phys. Rev. C **81**, 014901 (2010).
[50] R. A. Lacey *et al.*, Phys. Rev. C **81**, 061901 (2010).
[51] P. Staig and E. Shuryak, arXiv:1008.3139 [nucl-th].
[52] G.-Y. Qin, H. Petersen, S. A. Bass, and B. Muller, Phys. Rev. C **82**, 064903 (2010).
[53] M. L. Miller, K. Reygers, S. J. Sanders, and P. Steinberg, Annu. Rev. Nucl. Part. Sci. **57**, 205 (2007).
[54] T. Lappi and R. Venugopalan, Phys. Rev. C **74**, 054905 (2006).
[55] H.-J. Drescher and Y. Nara, Phys. Rev. C **76**, 041903 (2007).
[56] T. Hirano, U. W. Heinz, D. Kharzeev, R. Lacey, and Y. Nara, Phys. Lett. B **636**, 299 (2006).
[57] H.-J. Drescher, A. Dumitru, A. Hayashigaki, and Y. Nara, Phys. Rev. C **74**, 044905 (2006).
[58] B. Alver and G. Roland, Phys. Rev. C **81**, 054905 (2010).
[59] B. H. Alver, C. Gombeaud, M. Luzum, and J.-Y. Ollitrault, Phys. Rev. C **82**, 034913 (2010).
[60] H. Petersen, G.-Y. Qin, S. A. Bass, and B. Muller, Phys. Rev. C **82**, 041901 (2010).
[61] B. B. Back *et al.* (PHOBOS Collaboration), Phys. Rev. C **70**, 021902 (2004).

[62] Note that the event planes for the eccentricities are specified by the initial-state coordinate asymmetry, whereas the experimental event planes for v_n^* are specified by the final-state momentum space anisotropy. The two planes are correlated in ideal hydrodynamics.
[63] J. Adams *et al.* (STAR Collaboration), Phys. Rev. C **72**, 014904 (2005).
[64] P. Kovtun, D. T. Son, and A. O. Starinets, Phys. Rev. Lett. **94**, 111601 (2005).
[65] R. A. Lacey and A. Taranenko, in Proceedings of the Winter Workshop on Nuclear Dynamics, 2011.
[66] N. Borghini and J.-Y. Ollitrault, Phys. Lett. B **642**, 227 (2006).
[67] M. Csanad, T. Csorgo, and B. Lorstad, Nucl. Phys. A **742**, 80 (2004).